

Biochimica et Biophysica Acta, 506 (1978) 1–17 .

© Elsevier/North-Holland Biomedical Press

BBA 77891

ORGANOMETALLIC FATTY ACID AND PHOSPHOLIPID ANALOGS SYNTHESIS AND INCORPORATION AND DETECTION IN MODEL MEMBRANES AND BIOMEMBRANES

S. BRIAN ANDREWS ^{a,*}, J.W. FALLER ^b, RUSSELL J. BARNETT ^a and VINCI MIZUHIRA ^c

^a Section of Cytology, Yale University School of Medicine, ^b Department of Chemistry, Yale University, New Haven, Conn. 06510 (U.S.A.), and ^c Department of Cell Biology, Tokyo Medical and Dental University, Tokyo (Japan)

(Received June 20th, 1977)

Summary

1. To examine the potential of organometallic compounds as ultrastructural probes for the lipid organization of biomembranes, an organotin analog of palmitic acid, 12,12-dimethyl-12-stannahexadecanoic acid, was chemically synthesized. Subsequently, in vitro coupling of this synthetic fatty acid to egg lysophosphatidylcholine yielded an organotin analog of phosphatidylcholine.

2. This phospholipid was physically characterized by vesicle formation, nuclear magnetic resonance, agarose gel filtration, X-ray diffraction and differential scanning calorimetry, and the results were compared to the known properties of native egg phosphatidylcholine. The native and synthetic lipids were substantially similar regarding such fundamental properties as bilayer structure and dynamics and cation permeability. However, the unilaminar vesicle population of the organotin lipid assumed a larger mean diameter (390 Å) and width than did the comparable population of native lipid vesicles (230 Å).

3. Cultures of *Acholeplasma laidlawii*, grown in a medium supplemented with the organotin fatty acid, incorporated up to 39% of this label as esterified fatty acid into the phospholipids and glycolipids of the plasma membrane. Culture under these conditions did not impair the growth of these organisms.

4. Purified preparations of the plasma membrane of tin-enriched *A. laidlawii* were obtained. Conventional transmission electron microscopy revealed no differences in density between labeled and control membranes. In contrast, the tin label was readily detected by energy-dispersive X-ray microanalysis in an

* To whom correspondence should be addressed.

Abbreviations: AIBN, azobisisobutyronitrile; NMR, nuclear magnetic resonance.

analytical scanning electron microscope. Characteristic Sn $L\alpha$ X-rays, amounting to typically 7% of the total X-ray photons, and X-ray line pulse analysis data ("line scans") were obtained. Comparisons of this data with corresponding scanning secondary electron images indicated an absolute correlation between the density of Sn $L\alpha$ X-rays and images of membranes.

Introduction

Investigations of biological structure frequently require that the components of interest be marked for identification. For this reason, a labeling step is included in many studies utilizing microscopic [1,2] and spectroscopic [3,4] methods. The distribution of the label can be interpreted directly to reflect the native distribution of the labeled components, if the label is non-perturbing. However, there are certain biological structures for which this criterion is difficult to achieve. An example of such a structure is the lipid bilayer, in which the steric and electrostatic restrictions of the native structure are sufficiently severe that they effectively thwart most attempts to label the complex in the hydrophobic region without introducing extraneous interactions. In practice, this difficulty often occurs because most labeling techniques attach new molecules to the original structure. It is conceptually possible to minimize this constraint by using an analog-labeling approach rather than a tagging method; that is, labeling by replacement instead of by addition.

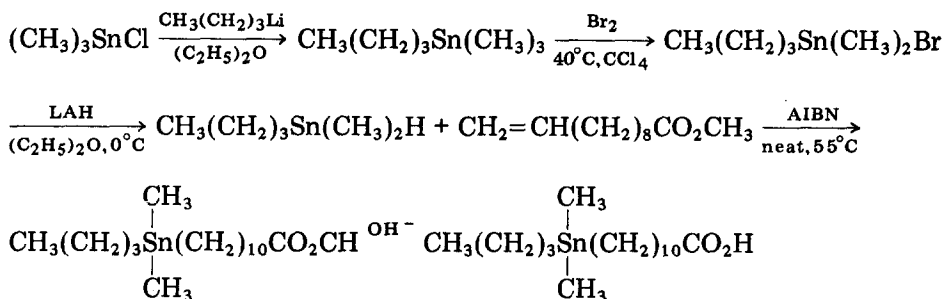
Organotin compounds are promising as analog labels for the bilayer region of membranes. These organometallics provide covalent bonds to carbon, a well-developed and versatile body of synthetic reactions and steric and electronic properties similar to the purely organic compounds from which they are derived [5]. Additionally, preliminary calculation suggested that, due to the relatively high atomic number of tin ($Z = 50$), a variety of electron microscopic techniques were potentially capable of detecting, identifying, and localizing this probe.

To test the ideas outlined above, an organometallic fatty acid, 12,12-dimethyl-12-stannahexadecanoic acid (compound I), and a phosphatidylcholine derivative of this (compound II) have been synthesized and characterized. Further, the organotin fatty acid has been incorporated into *Acholeplasma laidlawii* membranes in vivo, and detected in the analytical electron microscope. The results demonstrate a remarkable similarity of the tin fatty acid and phospholipid to natural lipid components of membranes thus supporting the proposition that organotin analogs are potentially useful labeling systems.

Methods and Materials

Synthesis of organotin lipids. The preparation of 12,12-dimethyl-12-stannahexadecanoic acid is outlined in Scheme 1. Trimethyltin chloride (Alfa Inorganics) was coupled with butyllithium (Alfa), followed by bromine cleavage [8] to yield butyldimethyltin bromide. This was reduced to the corresponding hydride via LiAlH_4 reduction [9]. Radical addition (azobisisobutyronitrile initiator) of this hydride to methyl Δ^{10} -undecenoate (from Δ^{10} -

Scheme I

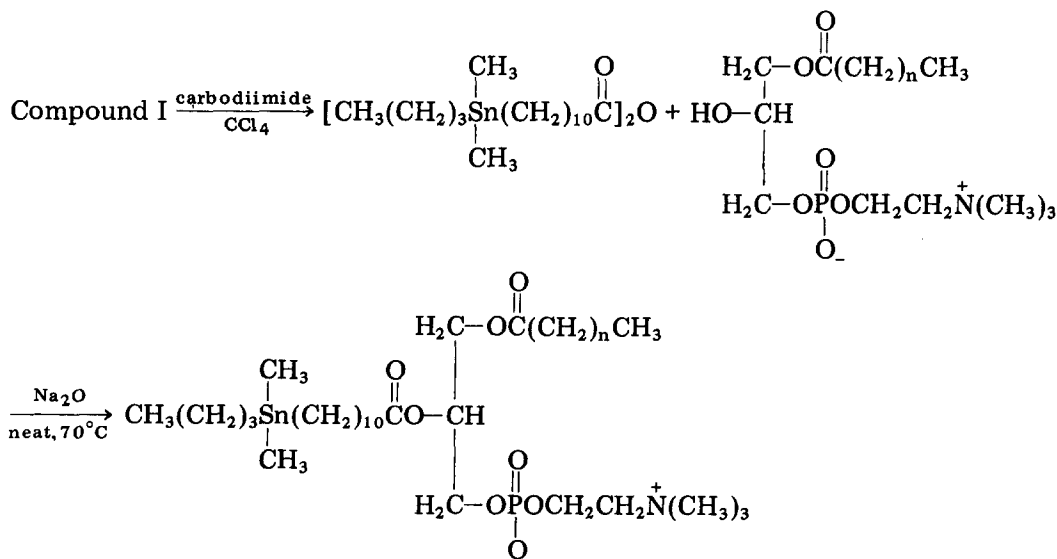


Compound I

undecenoic acid (Aldrich)) proceeded with specific addition of the organotin moiety to the terminal carbon [10], yielding the methyl ester of compound I. Subsequent base-catalyzed hydrolysis [11] gave the organotin fatty acid, compound I. This compound was purified by chromatography on silicic acid (hexane/benzene gradient elution), and this product exhibited a single spot on thin-layer chromatography (Bakerflex silica gel 1B-F, eluent light petroleum/ether/acetic acid (65 : 35 : 1, v/v)). The NMR and infrared spectra of the fatty acid (as well as the other new compounds in this sequence, viz., $\text{CH}_3(\text{CH}_2)_3\text{Sn}(\text{CH}_3)_2\text{H}$ and compound I-methyl ester) were fully consistent with the expected structure.

The phosphatidylcholine analog of the organometallic fatty acid was prepared as in Scheme 2. The acid was converted to the anhydride with dicyclo-

Scheme II



Compound II

hexylcarbodiimide [12]; egg lysolecithin was prepared by enzymatic hydrolysis of egg phosphatidylcholine [13] (from fresh eggs according to Papahadjopoulos and Miller [14]). These reagents were coupled by the method of Cubero Robles and Van den Berg [15] to afford compound II in virtually quantitative yield after chromatographic purification. The organotin phospholipid had a thin-layer R_F coincident with authentic phosphatidylcholine, and exhibited the NRM spectrum (deuteriochloroform and $[^2\text{H}_4]\text{methanol}$) expected for a phosphatidylcholine with chemically homogeneous (i.e. tin-labeled) β chains. The characterization and purity of compound II was further supported by gas-liquid chromatography of the constituent fatty acid methyl esters, obtained by acid- and base-catalyzed transesterification (F and M 402, 6 ft \times 1/8 inch 15% ethylene glycol succinate on Gaschrom P (Applied Sciences), oven temperature 180°C). A combination of literature procedures was employed [16,17] (cf. Results). In the present case, fatty acid composition was: organotin fatty acid (51%); stearic acid (14%); palmitic acid (33%); all others (4%).

Physical characterization of organotin phosphatidylcholine. Preparation of vesicles of egg and synthetic phosphatidylcholine was carried out as described previously [18], either in pure $^2\text{H}_2\text{O}$ or in 0.15 M KCl (H_2O or $^2\text{H}_2\text{O}$). NMR experiments, including lanthanide shift studies, were also performed as reported [18]. Occasionally, spectra were obtained with the aid of a computer of average transients. Gel filtration chromatograms were obtained from a Sepharose 2B column (2.5 \times 52 cm) using a continuous-flow differential refractive index monitor (Waters R-403). Differential scanning calorimetry was carried out using an instrument designed by J.M. Sturtevant, Department of Chemistry, Yale University.

Incorporation of the organotin fatty acid into the membranes of Acholeplasma laidlawii. *A. laidlawii* strain B was grown in a tryptose broth essentially as described by Razin et al. [19]. Cultures were inoculated with 5 ml of a previous 24-h culture (approx. $5 \cdot 10^9$ cells), and allowed to grow to the peak of logarithmic phase, which was typically 24 h with a density of 10^9 cells/ml. Growth was monitored by the increase in turbidity at 410 nm. To prepare a fatty acid-supplemented medium, the fatty acid (50 mg/ml in absolute ethanol) was added to the culture flask and swirled to coat the vessel walls. Subsequently, acetone-defatted bovine serum albumin was added and similarly swirled to adsorb the free fatty acid. The normal culture broth then was added and inoculated as usual. Cultures were grown unsupplemented with 1 ml of ethanol added, and supplemented with oleic acid or fatty acid I at concentrations of 25 and 50 mg/l.

At the end of the logarithmic phase of growth, the cells were harvested and membranes were isolated as described elsewhere [19]. The membranes were further purified according to Terry et al. [20], and the final preparation was stored as a frozen pellet. Alternatively, these membranes were washed twice in 0.17 M $(\text{NH}_4)_2\text{CO}_3$ (pH 7.4) before storage.

For fatty acid analysis, phospholipids and glycolipids were extracted from membrane preparations in the standard manner, using chloroform/methanol (2 : 1, v/v). Transesterification ($\text{BF}_3/\text{methanol}$) and gas-liquid chromatographic analysis were as described above. The following fatty acids were assayed: $\text{C}_{14:0}$, $\text{C}_{16:0}$, $\text{C}_{16:1}$, $\text{C}_{18:0}$, $\text{C}_{18:1}$, and compound I; all others were present at levels of

2% or less. Relative amounts of fatty acids are reported as area-%, since the detector response factors for all esters, including compound I-methyl ester, were approx. 1.0.

Electron microscopy and X-ray microanalysis. For conventional transmission electron microscopy, pellets of isolated control and experimental ghosts were suspended in distilled water and a microdrop was pipetted onto a carbon-coated copper grid; both unfixed ghosts and those fixed in 2% phosphate-buffered glutaraldehyde were used. Alternatively, pellets of ghosts were fixed in 2% glutaraldehyde and embedded either in a glutaraldehyde-carbohydrazide copolymer [21], a water-miscible embedding medium that retains phospholipids (92%), or in Epon (after dehydration through a graded series of alcohols). Sections were prepared on an LKB Ultratome and examined with a modified Hitachi HU-11E electron microscope provided with a cold stage and vac-ion and cryopumps to reduce contamination. Some of the sections were stained with uranyl acetate and lead citrate in the conventional manner to provide membrane contrast.

For experiments involving scanning electron microscopy, scanning transmission electron microscopy and X-ray microanalysis, resuspended pellets of control and experimental ghosts were used, as well as sections as described above. A microdrop was pipetted onto a handmade, clean carbon plate or onto carbon-coated copper, nylon or aluminum grids, and air-dried at room temperature. The specimens were observed in a JEM-100C analytical microscope fitted with a goniometer stage, an ASID-4 scanning device, and an EDAX-707B energy-dispersive X-ray spectrometer accessory. Electron micrographs were taken as the scanning secondary electron image at 10–40 kV with a beam current of 10^{-11} A and a spot size of 70 nm. For obtaining secondary X-ray emission spectra, samples were tilted 30–45° to the electron beam to optimize the X-ray take-off angle and illuminated for 100 s. Typically, an accelerating voltage of 10 kV, an illuminating current of $2.5 \cdot 10^{-10}$ A, and a spot size of 100–150 nm were used. In the case of X-ray line pulse analysis (line scans), the conditions were as described above for the scanning secondary electron image.

Results

Chemical synthesis and analysis of the organotin fatty acid and phospholipid

The synthesis of the organotin fatty acid is a straightforward adaptation of well-known chemical routes, as indicated in Methods and Materials; this also holds for the phospholipid analog. All steps in the preparation of the fatty acid proceeded in satisfactory yield, typically 60–85%. The overall yield based on organotin groups was 11%; no attempt was made to optimize yields. The placement of the organometallic moiety at the 12-position was a matter of convenience, since both *n*-butyllithium and Δ^{10} -undecenoic acid (a constituent of castor oil) were commercially available. However, the synthetic scheme is sufficiently versatile to allow the preparation of isomers of this compound (and of analogs with longer or shorter chains) with the metal anywhere except the 1-, 2- or terminal positions. Routes to the appropriate alkylolithiums [22] and Ω -unsaturated fatty acid esters [23] are available. Gas-liquid chromatography analysis of the fatty acid compositions of the tin-labeled phosphatidylcholine

required a modification of the standard analysis procedure [16], since at the usual analytical conditions the methyl ester of the tin fatty acid had a retention time virtually identical to that of methyl oleate. This difficulty could be circumvented by a difference analysis. The organotin derivative is quantitatively degraded by C-Sn bond cleavage under acid-catalyzed transesterification conditions, as expected [6]; thus, only methyl oleate is detected by subsequent gas-liquid chromatographic analysis. However, the organometallic fatty acid is stable to base-catalyzed procedures [11], and this method detects both compound I-methyl ester and methyl oleate as a single symmetrical peak. The relative amount of organotin label in the phospholipids of interest may be readily determined by the difference of these values. No other peculiarities were encountered in the preparation and manipulation of these analogs.

Comparison of the physical characteristics of native and synthetic phosphatidylcholine

To determine that the organotin phospholipid was a biologically relevant analog, certain of its physical properties were compared to egg phosphatidylcholine. Unilamellar phospholipid vesicles are widely recognized as a simple model system for the phospholipid component of biomembranes. These vesicles are closed, bilayer structures that present many of the salient features of native membranes, and offer the additional advantages of being reproducible and relatively homogeneous [24]. If the metal-labeled phospholipid is subjected to the usual condition of ultrasonic irradiation, vesicles are formed in a manner analogous to that of native lecithin. Qualitatively, the synthetic material differs from the native phosphatidylcholine in this procedure in that the tin lipid requires longer times (approx. 50%) to complete vesicle formation at comparable conditions of concentration and sonic power. Also, final suspensions of the organotin vesicles are somewhat more turbid than are those of native lipid. Increased turbidity would be expected if the metal-labeled vesicles are larger than vesicles of egg phosphatidylcholine, and this is consistent with the data below.

NMR is a particularly useful tool for comparing the physical nature of vesicles. Chemical shifts (δ) provide an indication of the structure and environment of component phospholipids, and linewidth values ($\nu_{1/2}$) similarly reflect the motional state of observable molecular segments [25]. Moreover, lanthanide shift techniques allow a straightforward estimate of the average size of these aggregates [18]. Corresponding 100 MHz ^1H NMR spectra of native and labeled phosphatidylcholine vesicles are illustrated in Figs. 1B and 1D. The details of these spectra correlate closely when allowances are made for the expected chemical shift differences induced by the organotin group. Thus, the chemical shifts of resonances which these phospholipids have in common are identical, viz. $-\text{N}(\text{CH}_3)_3$, $-\text{NCH}_2-$, $-\text{POCH}_2-$, $\alpha\text{-CH}_2$, chain CH_2 and terminal CH_3 . The three resonances apparent in Fig. 1B but absent in Fig. 1D are the result of unsaturation in the native lipid; they are not expected for the synthetic material. The sharp singlet at 0.06 ppm is assigned to the $-(\text{CH}_3)_3\text{Sn-}$ protons; the chemical shift, as well as the sidebands ($J_{^{117}\text{Sn}, ^{119}\text{Sn-H}} = 52 \text{ Hz}$), are as expected for an alkyltin derivative [7] *.

* In the case of the tin phospholipid, the intensity of the terminal CH_3 resonance is enhanced somewhat at the expense of the chain methylene envelope. This is attributable to the expected appearance of the chain methylenes α to tin at 1 ppm; that is overlapping the terminal CH_3 resonance.

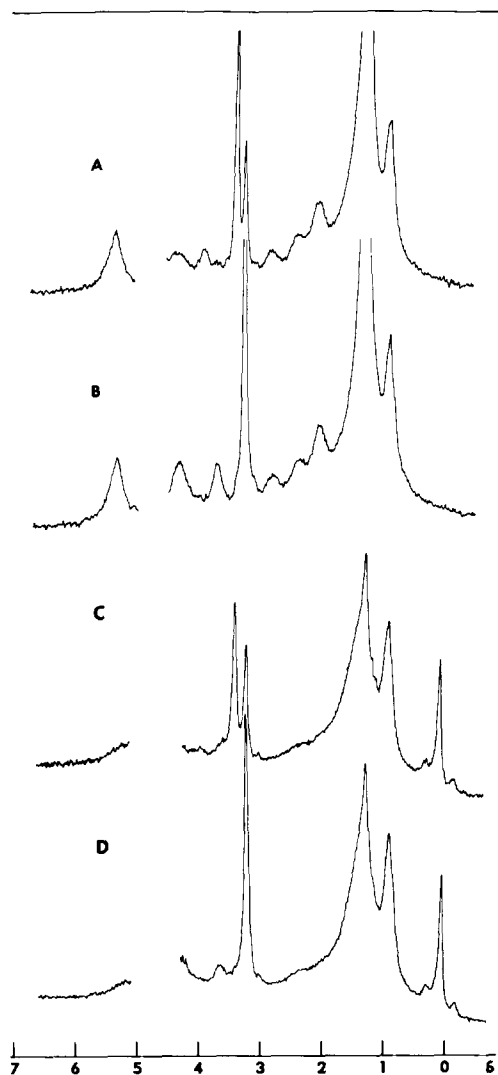


Fig. 1. 100 MHz ^1H NMR spectra of 36 mM egg phosphatidylcholine vesicles in the presence (A) and absence (B) of 1.2 mM Pr^{3+} . Corresponding spectra of approx. 20 mM organotin phosphatidylcholine vesicles in the presence of 1.6 mM Pr^{3+} (C) and lanthanide free (D). Assignments are as in ref. 26 and the text.

Regarding motional characteristics, estimates based on linewidths indicate substantial similarity, both in the hydrophobic and hydrophilic regions. In particular, $\nu_{1/2}(\text{NMe}_3)$ is 6 Hz for egg phosphatidylcholine and 7 Hz for tin phosphatidylcholine. While linewidths are insufficient to adequately assess the relaxation characteristics of weak or overlapping resonances, a qualitative comparison of these resonance shapes implies a motional similarity. The full width at half-height, $\nu_{1/2}[-(\text{CH}_3)\text{Sn-}]$, is 9 Hz, suggesting a transverse relaxation time in agreement with that anticipated for a vesicle methyl rotor, e.g. 36 ms for the terminal methyl groups of sonicated native phospholipid [27].

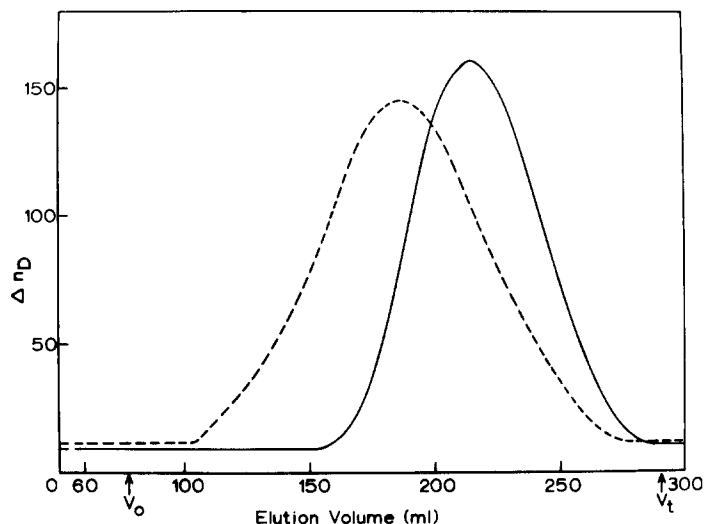


Fig. 2. Differential refractive index profile (arbitrary units) of vesicles of native lipid (—) and tin-labeled lipid (----) chromatographed on a Sepharose 2B column (2.5 × 52 cm).

The effect of small amounts of aquated Pr^{3+} on the spectra of native and labeled vesicles is shown in Figs. 1A and 1C, respectively. The results, similar in both cases, is a splitting of resonances derived from hydrophilic residues into two components. The more intense resonance of a pair, shifted downfield in this case, is assigned to moieties lying at the exterior interface of the closed bilayer vesicles; the less intense, unshifted counterpart occupies the interior hydrophilic surface [18]. The bilayer must be impermeable to cations to exhibit this effect. Hydrophobic resonances are not affected, except for a slight broadening, by the presence of Pr^{3+} in concentrations as high as 50 mM. The failure of lanthanide ions to perturb the $-(\text{CH}_3)_2\text{Sn}-$ resonance at high concentrations (not illustrated) is unequivocal evidence that the organotin moiety resides in the fatty acid region. This conclusion is supported by X-ray data. The low angle X-ray diffraction pattern and electron density profile of vesicles of the organotin phospholipid above the phase transition are indistinguishable from that of native phosphatidylcholine vesicles [28] (Wise, D.S. and Engelman, D.M., personal communication). In particular, both diffraction patterns show maxima corresponding to a 36 Å trans-bilayer spacing*.

The lanthanide ion-induced shift technique is also useful for obtaining a straightforward estimate of vesicle size. Assuming a bilayer width of 36 Å and equal surface area per headgroup, the outside/inside mol ratio, obtained by integration of the $-\text{N}(\text{CH}_3)_3$ resonances, provides the average, aggregate diameter by geometry [18,29]. For vesicles of native lipid, an outside/inside ratio of 2.12 implies a diameter of 230 Å, in good agreement with values reported previously for unfractionated dispersions [29,30]. In the case of the

* Fourier analysis of the diffraction pattern of tin-labeled vesicles did not reveal additional electron density in the hydrophobic region attributable to the metal. However, the mechanisms and conditions of scattering are quite different for X-rays and (elastic) electrons, and this observation has no necessary implications for the prospects of this label as an electron microscopy probe.

organometallic lipid, a ratio of 1.50 gives a calculated vesicle diameter of 390 Å.

The size differential between these two vesicle dispersions is also apparent in agarose gel filtration experiments. The elution pattern of native lipid vesicles shown in Fig. 2 is substantially similar to previous reports (e.g. Refs. 29, 30 and 32) although a peak at V_0 is not apparent in this case because larger lipid aggregates, which usually elute at V_0 , had been previously removed by centrifugal purification, and because the differential refractive index detection method employed here is not excessively sensitive to large structures as is the turbidity detection method more commonly used. The chromatographic profile of sonicated suspensions of the organotin lipid is consistent with a monophasic distribution of unilaminar vesicles. However, these vesicles exhibit a shift to lower elution volumes, as expected for larger aggregates, and also a marked increase in the size distribution, as implied by the peak width. Column calibration has generally led to an estimate of approx. 250 Å for the mean diameter of unilaminar phosphatidylcholine vesicle preparations. However, detailed analysis of elution profiles and careful calibration of the column used here (Andrews, S.B., unpublished) gave a somewhat smaller mean diameter, viz. 230 Å, for unfractionated egg phosphatidylcholine dispersions. Gent and Prestegard [31] have recently reported a similar value. In contrast, the mean diameter of the labeled vesicles was 330 Å *.

The crystalline-liquid crystalline phase transition of a coarse suspension of organometallic phospholipid was not found above 0°C, as expected for a phospholipid which possesses heterogeneity of fatty acid content and/or steric deviation from saturated straight chains. The transition for native phosphatidylcholine is also below 0°C [33].

In vivo incorporation of the tin fatty acid into cell membranes

Membranes of *A. laidlawii* B may be selectively enriched in a chosen fatty acid constituent by culture in a defined medium [34]. This system has been used by Tourtellotte et al. [35] to demonstrate the biological compatibility of spin-labeled fatty acids. When such a culture was carried out with the organotin fatty acid, *A. laidlawii* incorporated this compound into its phospholipids and/or glycolipids. Unsupplemented control cultures, with or without ethanol added, grew to maximum density (10^9 /ml) in approx. 24 h. No statistically significant difference in either growth rate or final cell density was observed for cultures supplemented with oleic acid or tin fatty acid at a level of 25 mg/l. The presence of the tin fatty acid in the membranes of these organisms had no apparent effect on the viability of these cells. Likewise, membranes could be isolated from the tin-enriched organisms without incident. The level of incorporation of label, as determined by gas-liquid chromatographic analysis, was 27.5% of total fatty acids for supplementation at 25 mg/l, and 39.4% at 50 mg/l. Higher levels of supplementation were not investigated. No dramatic difference in the relative amounts of the normal fatty acid constituents was noted, although myristic acid was consistently lower than expected (9.0% at

* The differing values for mean diameter of organotin vesicles obtained by NMR and permeation chromatography are probably not inconsistent. The two methods report physically different "averages", and both values can represent the same population of vesicles if the width of the distribution is appropriate.

25 mg/l, 3.6% at 50 mg/l). However, it is not possible to reasonably draw any inferences regarding selectivity of labeled fatty acid replacement in this system, since the ratios of normal fatty acids vary widely from batch to batch. Only two obvious differences between normal and tin-enriched membranes were observed in these manipulations; the amount of carotenoid pigment was apparently reduced in the supplemented membranes, as judged by the lower intensity of orange-yellow color, and the supplemented membranes may be somewhat more mechanically fragile, as implied by the more frequent occurrence of membrane fragments seen during electron microscopy.

Electron microscopy and X-ray microanalysis

Isolated, tin-supplemented *A. laidlawii* membrane ghosts were examined by transmission electron microscopy at 50 and 100 kV. No clear-cut differences in density could be readily distinguished between experimentals and controls subjected to the same beam exposure and photographic development. The same result occurred in sections of pellets of ghosts, fixed in glutaraldehyde and embedded in the glutaraldehyde-carbohydrazide copolymer [21], which

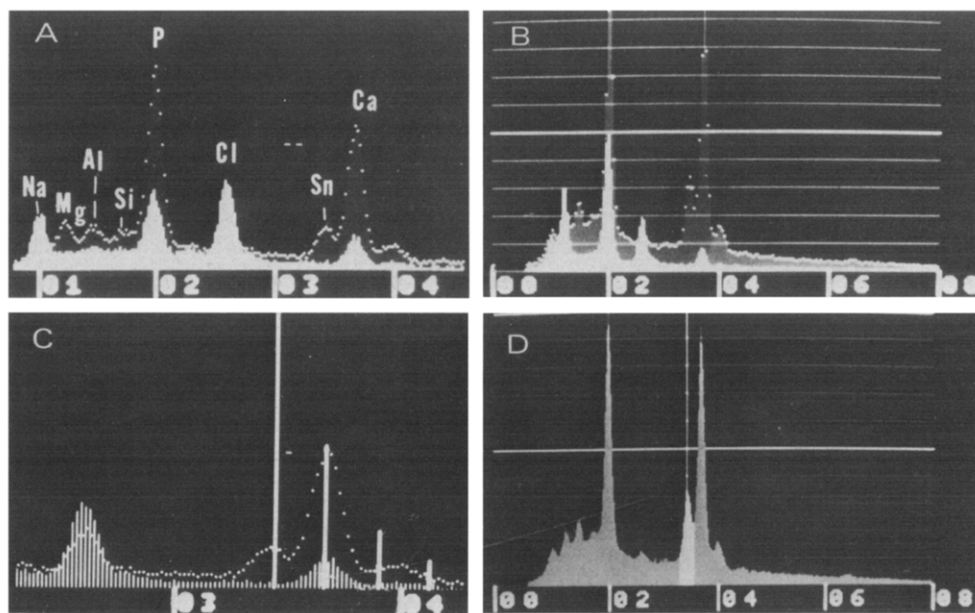


Fig. 3. Characteristic X-ray emission spectra of *A. laidlawii* membrane preparations. All spectra were accumulated for 100 s at a resolution of 20 eV/channel. The abscissa is calibrated in keV, and the ordinate is either 2500 (A and C) or 5000 (B and D) counts full scale per channel. Irradiation conditions are described in Methods and Materials, and the approximate, relative integrated areas as gross (uncorrected) counts/s are given below in parentheses. (A) X-ray spectra of tin-labeled membranes (dotted, 800) superimposed on the spectrum of control membranes (solid, 350) from a parallel culture. The elemental assignments are indicated. (B) Spectra of a different preparation of labeled (dotted, 2100) and unlabeled (solid, 800) membranes. These may be compared to A. (C) A horizontal scale expansion of A. The cursors indicate the expected positions and relative intensities of the Sn L emissions. The lowest energy Sn L $\alpha_{1,2}$ line is at 3440 eV. (D) Spectrum of tin-labeled ghosts, illustrating in white the energy window, centered on the cursor at 3420 eV, used to obtain the line pulse analysis data of Figs. 4 and 5. The window contained 162 counts/s as compared to 2200 counts/s for the entire spectrum.

retained over 90% of the phospholipids. Such sections stained with uranyl acetate and lead citrate produced stained lamellae surrounding a clear central lamella of 40 Å, and the total plasma membrane width measured 90 Å in both experimentals and controls.

Isolated ghosts were more readily apparent in scanning electron micrographs. The labeled ghosts occurred singly or in clumps and appeared normal; however, fragments of membranes were also often observed. Numerous X-ray emission spectra were obtained from several experiments over a period of 2 years. With experimental ghosts, the gross X-ray counts per 100 s ranged from 17 300 to 221 000. The following elements were identified by their $K\alpha$ (and occasionally $K\beta$) lines: Na, Mg, Al, Si, P, Cl, and Ca. In most cases phosphorus and calcium were the most abundant elements (Fig. 3A). Tin was identified by the $Sn L\alpha_{1,2}$ emission at 3340 eV, which typically accounted for 7% of the gross counts, and

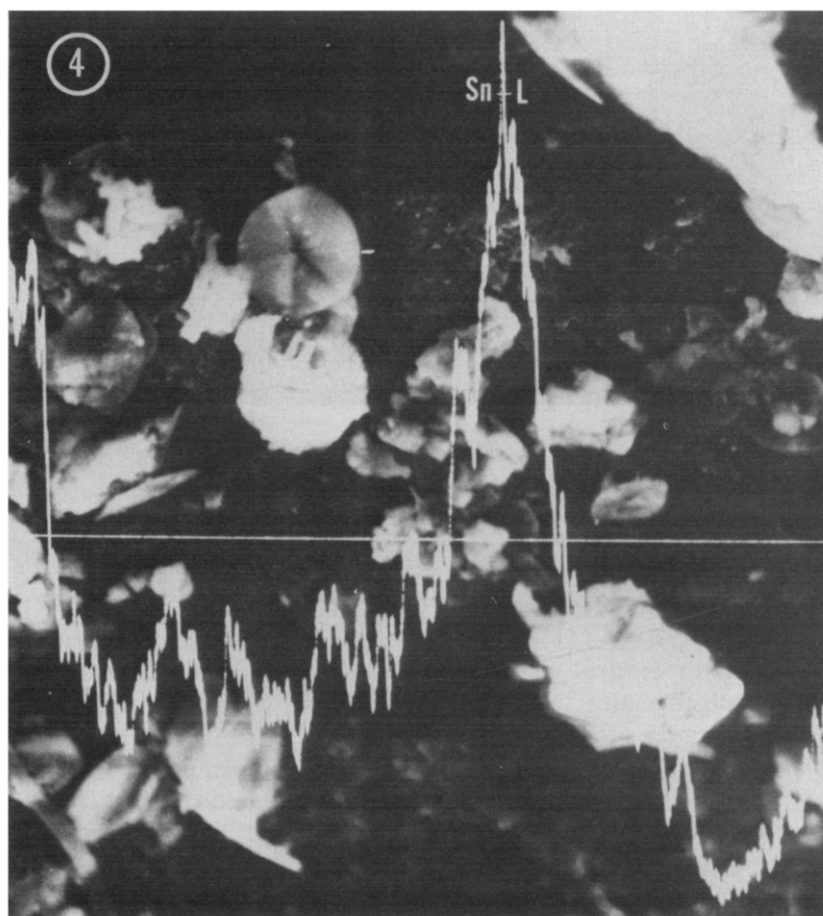


Fig. 4. Scanning secondary electron micrograph of a preparation of tin-labeled *A. laidlawii* membranes and membrane fragments. The membranes are supported on a handmade carbon block. The X-ray line pulse spectrum obtained from the energy window shown in Fig. 3D, is superimposed. The horizontal line indicates the plane of the X-ray scan. Magnification, $\times 6400$.

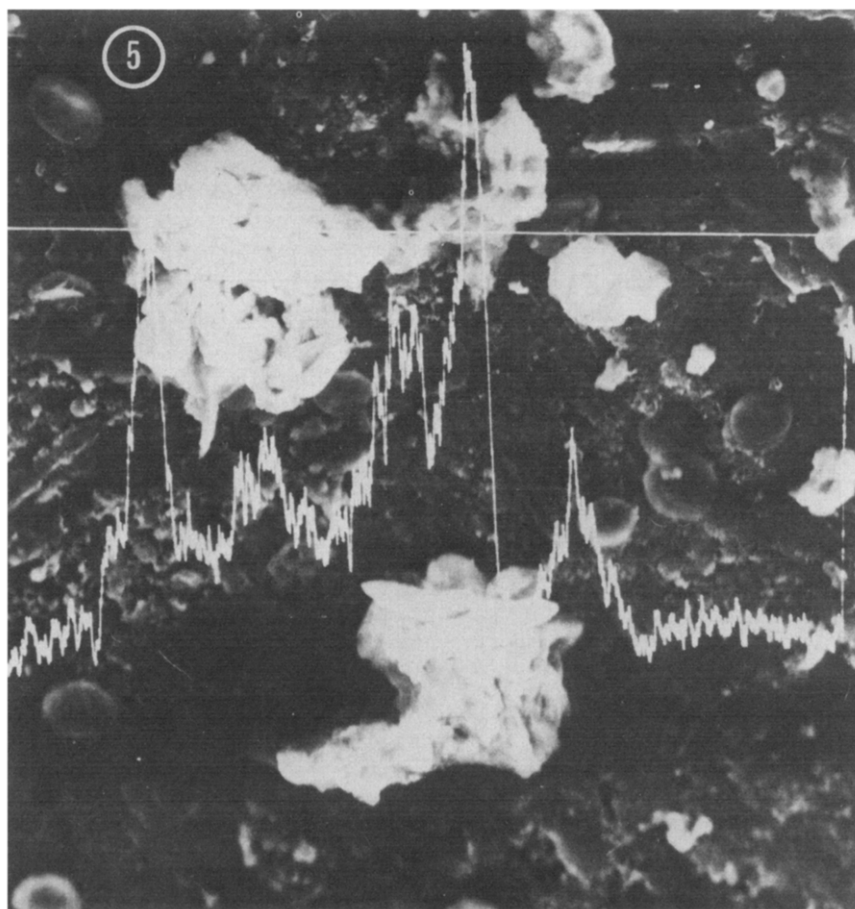


Fig. 5. As in Fig. 4, a scanning micrograph and X-ray line pulse spectrum of a different membrane preparation. Magnification, $\times 2500$.

was at least three times higher than the background noise. This line was just to the low-energy side of the Ca $K\alpha$ emission (3690 eV), and the Ca $K\alpha$ and $K\beta$ lines obscured the other characteristic emissions of tin at 3660 eV ($L\beta_{1,3}$), 3900 eV ($L\beta_2$) and 4130 eV ($L\gamma$) (Fig. 3C). Invariably, fewer total counts were accumulated in 100 s on control ghosts (15 000–70 000); the difference is attributable to the substantially lower concentrations of calcium and phosphorus, and the total absence of tin (Figs. 3A and 3B) *.

In a number of experiments, the X-ray spectrometer was arranged to accept emissions only from a "Sn window", centered as 3440 eV, as shown in Fig. 3D. This allowed the accumulation of Sn $L\alpha_{1,2}$ X-rays as a function of spatial distribution in the specimen. This procedure is known as X-ray line pulse analysis or line scanning. Typical examples of such line scans, superimposed on

* Recently, the organotin phospholipid was detected by X-ray microanalysis using stationary spot techniques in thin sections of these membranes embedded in glutaraldehyde-carbohydrazide and viewed in cross-section in a Siemens ST100F scanning transmission electron microscope equipped with a Kevex 5100 energy-dispersive X-ray spectrometer.

the corresponding scanning images, are illustrated in Figs. 4 and 5. In all cases, there was an obligatory association of statistically significant, tin-derived X-ray emissions with membrane ghosts, thus substantiating the incorporation determined with chemical methods.

Discussion

Organotin derivatives possess a number of advantages that make them attractive for studying the feasibility of analog labeling for electron microscopy. The tin-labeled fatty acid and membrane contain a covalently bonded metal tag stable to *in vivo* and analytical conditions. These bonds are resistant to hydrolysis, thermolysis, oxidation and other adventitious reactions which might compromise localization. The label is by its nature specific. It makes a minimum compromise with structural and chemical similarity since the $-(CH_3)_2Sn-$ moiety has the same sp^3 -tetrahedral geometry as the carbon it replaces, similar bond lengths, and no extraneous Lewis acid or base characteristics. The relatively minimal steric requirement of the organometallic moiety is illustrated in Fig. 6. It is apparent that the size of the label is roughly the same as that of a natural, unsaturated fatty acid, and significantly less than that of a representative "spin label."

Concerning the ability of these organometallic labels to serve as analogs for native membrane constituents, a comparison of the physical properties of tin-

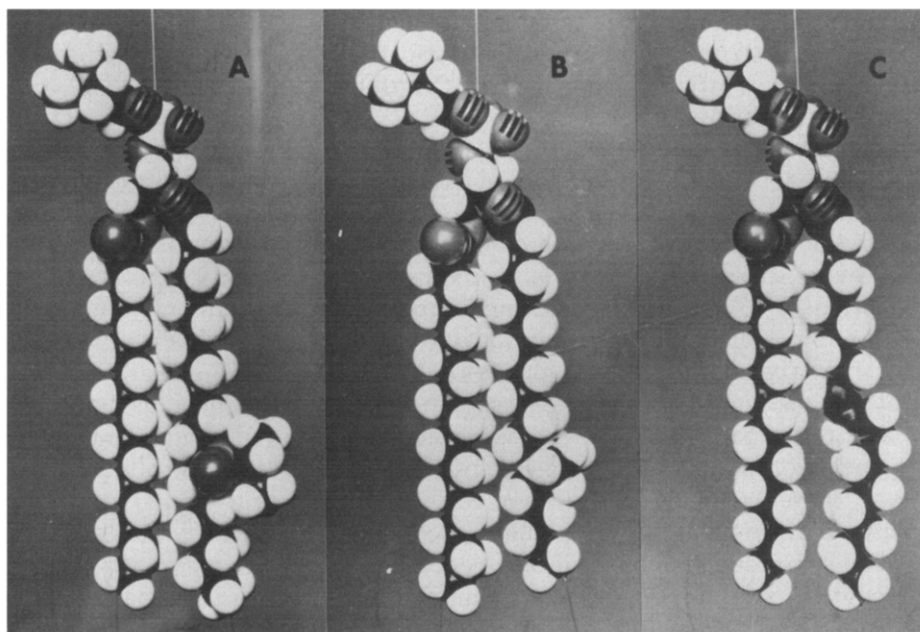


Fig. 6. CPK models of phosphatidylcholine. The β fatty acids are: (A) a representative spin label, the *N*-oxyl-4',4'-dimethyloxazolidine derivative of 12-ketostearic acid [13,36]; (B) the organotin fatty acid; and (C) oleic acid in a β -coupled configuration.

labeled and natural phosphatidylcholine shows many excellent correlations. Both species form single-shelled vesicles under the appropriate conditions, display the proper structural and motional characteristics, and are indistinguishable on the basis of cation permeability and metal-ion binding. The X-ray diffraction and NMR data demonstrate that the bilayer arrangement of the model membranes remains intact in the labeled system. The only obvious departure from physical similarity found in these experiments is the difference in vesicle size and distribution, as determined by NMR and permeation chromatography. Although it is well-known that fatty acid variations can modify the molecular packing characteristics of membranes [37–39], these usually appear to be less influential than headgroup structure in determining vesicle size parameters. Therefore, the observation of a fatty acid-dependent deviation in this system probably represents a real difference in the thermodynamics of vesicle formation. It is not clear, however, that this apparently minor difference will be important in membranes of heterogeneous composition which will have been labeled with low-to-moderate concentrations of this probe. Lastly, the ability of *A. laidlawii* to grow in a tin-supplemented medium, and to incorporate this label into the phospholipids and glycolipids of a functional membrane implies an additional degree of similarity between the organotin fatty acid and native fatty acids. This system has not been investigated for selectivity in the replacement of native fatty acids, or for a preference for specific headgroups. However, recent studies have been carried out on the incorporation of the tin fatty acid into the phospholipid of confluent cultures of A549 cells. This cell line, a human adenocarcinoma presumably derived from the pulmonary Type II cell responsible for surfactant synthesis [40], normally utilizes substantial amounts of fatty acids, particularly palmitate, for the synthesis of new membrane and secretory product. In this system the organotin fatty acid exhibits a considerable preference to substitute for palmitate (Nardone, L.L., Andrews, S.B. and R.J. Barnett, unpublished).

Electron-scattering calculations [41,42] performed early in the course of this study, and based on the composition of *A. laidlawii* membranes and a 35% labeling efficiency suggested that scattering enhancement due to tin should be readily detectable in the elastic (dark-field) image, and in the elastic/inelastic ratio. However, these calculations also indicated that detection in the conventional bright-field mode was a marginal proposition, feasible only with considerable technical difficulty and very favorable specimens. Thus, it was not surprising that labeled and control ghosts on thin (approx. 50 Å) carbon films could not be distinguished by photographic density differences using transmission electron microscopy. These experiments employed controlled beam exposure and photographic development, but were otherwise conventional.

However, these experiments did serve to show that there were no detectable ultrastructural differences between these specimens. In contrast, the tin label was expected to be readily detectable using energy-dispersive X-ray spectrometry and an analytical scanning/scanning transmission electron microscope and this was the case. The results reported here are as yet insufficient to assess the potential of X-ray microanalysis for the localization of organotin probes in biological experiments, since a number of questions remain unanswered. In particular, the minimum detectable limit of the tin label has not been deter-

mined and the spatial resolution is not known *. Furthermore, although X-ray microanalysis has been employed effectively in biological systems in which circumstance provided a high local concentration of the element(s) of interest [47–51], the low inherent collection efficiency of X-ray detectors is more of a limitation in experiments where the concentrations of label is also low. The present experiments do demonstrate, however, that the photoelectric cross-section of tin is sufficiently high to guarantee detection with much greater sensitivity or resolution using an energy-loss spectrometer [52]. An alternative possibility for the microscopic detection of the organotin probe is the high-resolution scanning transmission electron microscope which employs differential detectors for elastically and inelastically scattered electrons [53]. The calculations mentioned above indicate that this microscope should be effective in the dark-field and ratio modes, and preliminary experiments along these lines have been encouraging.

Regarding the potential value of ultrastructural lipid probes, the importance, diversity and complexity of phospholipid distribution in functional membranes is becoming increasingly apparent. Lipid trans-membrane asymmetry [54] and specific, functionally important lipid-protein interactions [55] have been demonstrated biochemically in native membranes, and there are suggestions from model system studies that in-plane lipid heterogeneity may be a common feature of membranes at physiological temperatures as well [56]. Considering the dynamic and time-dependent nature of phospholipid distributions in bilayers, ultrastructural methods for the study of lipid localization very clearly become desirable.

A further application of this probe concerns the study of newly formed membranes or lipid-containing secretory products, as exemplified by our current efforts with the cultured A549 cell system described above. Additional studies to define further the capabilities and limitations of organometallic lipid probes are clearly required and these focus presently on improved electron microscopy methodology and the development of specificity in the incorporation of these probes into various biomembranes. The results reported here suggest that appropriately labeled heavy metal probes can be used to investigate surface topography of isolated membrane systems and support the possibility that this strategy can be extended to other specific constituents of membranes.

Acknowledgements

The authors acknowledge U.S.P.H.S. Grants AM 03688, GM 00105, and N.S.F. Grant GP-36485, and the donors of the Petroleum Research Fund, administered by the A.C.S., for support of this research. We are further grateful to Professor J.M. Sturtevant, Yale University, who carried out the differential scanning calorimetry, to Professor J.M. Gilliam, University of Oklahoma Medical Center, for assistance in culturing *A. laidlawii* and harvesting the

* A 70 nm spot was used in these experiments. However, the actual resolution may be somewhat less than this, depending on the specimen thickness and other factors [43,44]. Also, the possibility that Sn $L\alpha$ emissions may have been artificially enhanced in these particular preparations as a result of secondary fluorescence induced by high calcium levels [45,46] is not likely, since the isolated membrane specimens were thin.

plasma membranes, and to Dr. Y. Futaesaku, Tokyo Medical and Dental University, who aided us considerably in some of the X-ray microanalysis experiments. Lastly, we thank the JOEL Co. (U.S.A.), Medford, Mass., and Siemens AG, Karlsruhe, German Federal Republic, for the use of their analytical microscopes for certain of the experiments.

References

- 1 Sternberger, L.A. (1974) *Immunocytochemistry*, Chapters 2, 3, and 5, Prentice-Hall, Englewood Cliffs, N.J.
- 2 Davis, W.C. (1974) *Methods Enzymol.* 32, 60—70
- 3 Chapman, D. and Dodd, G.H. (1971) in *Structure and Function of Biological Membranes* (Rothfield, L.I., ed.), pp. 67—68, Academic Press, New York
- 4 Jost, P., Waggoner, A.S. and Griffith, O.H. (1971) in *Structure and Function of Biological Membranes* (Rothfield, L.I., ed.), pp. 140—141, Academic Press, New York
- 5 Neumann, W.P. (1970) *The Organic Chemistry of Tin*, Chapters 2 and 4, Wiley and Sons, New York
- 6 Neumann, W.P. (1970) *The Organic Chemistry of Tin*, p. 34, Wiley and Sons, New York
- 7 Neumann, W.P. (1970) *The Organic Chemistry of Tin*, p. 222, Wiley and Sons, New York
- 8 Rosenberg, S.D., Debreczeni, E. and Weinberg, E.L. (1959) *J. Am. Chem. Soc.* 81, 972—975
- 9 Kuivila, H.G. and Beumel, Jr., O.F. (1961) *J. Am. Chem. Soc.* 83, 1246—1250
- 10 Neumann, W.P., Niermann, H. and Sommer, R. (1962) *Justig Liebigs Ann. Chem.* 659, 27—39
- 11 Van der Kerk, G.J.M. and Noltes, J.G. (1959) *J. Appl. Chem.* 9, 113—120
- 12 Selinger, Z. and Lapidot, Y. (1966) *J. Lipid Res.* 7, 174—175
- 13 Hubbell, W.L. and McConnell, H.M. (1971) *J. Am. Chem. Soc.* 93, 314—326
- 14 Papahadjopoulos, D. and Miller, N. (1967) *Biochim. Biophys. Acta* 135, 624—638
- 15 Cubero Robles, E. and Van den Berg, D. (1969) *Biochim. Biophys. Acta* 187, 520—526
- 16 Morrison, W.R. and Smith, L.M. (1964) *J. Lipid Res.* 5, 600—608
- 17 Marinetti, G.V. (1962) *Biochemistry* 1, 350—353
- 18 Andrews, S.B., Faller, J.W., Gilliam, J.M. and Barnett, R.J. (1973) *Proc. Natl. Acad. Sci. U.S.* 70, 1814—1818
- 19 Razin, S., Morowitz, H.J. and Terry, T.M. (1965) *Proc. Natl. Acad. Sci. U.S.* 54, 219—225
- 20 Terry, T.M., Engelman, D.M. and Morowitz, H.J. (1967) *Biochim. Biophys. Acta* 135, 381—390
- 21 Heckman, C.A. and Barnett, R.J. (1973) *J. Ultrastruct. Res.* 42, 156—179
- 22 Brown, T.L. (1965) *Adv. Organometal. Chem.* 3, 365—395
- 23 Ansell, M.F., Emmett, J.C. and Coombs, R.V. (1968) *J. Chem. Soc. C*, 216—225
- 24 Huang, C. and Thompson, T.E. (1974) *Methods Enzymol.* 32, 485—489
- 25 Horwitz, A.F. (1972) in *Membrane Molecular Biology* (Fox, C.F. and Keith, A.D., eds.), pp. 164—191, Sinauer, Stamford, Conn.
- 26 Finer, E.G., Flook, A.G. and Hauser, H. (1971) *FEBS Lett.* 18, 331—334
- 27 Horwitz, A.F., Horsley, W.J. and Klein, M.P. (1972) *Proc. Natl. Acad. Sci. U.S.* 69, 590—593
- 28 Wilkins, M.H.F., Blaurock, A.E. and Engelman, D.M. (1971) *Nat. New Biol.* 230, 72—76
- 29 Sheetz, M.P. and Chan, S.I. (1972) *Biochemistry* 11, 4573—4581
- 30 Andrews, S.B., Hoffman, R.M. and Borison, A. (1975) *Biochem. Biophys. Res. Commun.* 65, 913—919
- 31 Gent, M.P.N. and Prestegard, J.H. (1974) *Biochemistry* 13, 4027—4033
- 32 Huang, C. (1969) *Biochemistry* 9, 344—351
- 33 Ladbrooke, B.D., Williams, R.M. and Chapman, D. (1968) *Biochim. Biophys. Acta* 150, 333—340
- 34 McElhaney, R.M. and Tourtellotte, M.E. (1969) *Science* 164, 433—434
- 35 Tourtellotte, M., Branton, D. and Keith, A.D. (1970) *Proc. Natl. Acad. Sci. U.S.* 66, 909—916
- 36 Keith, A.D., Waggoner, A.S. and Griffith, O.H. (1968) *Proc. Natl. Acad. Sci. U.S.* 61, 819—826
- 37 Demel, R.A., Guerts van Kessel, W.S.M. and van Deenen, L.L.M. (1972) *Biochim. Biophys. Acta* 266, 26—40
- 38 Jendrasiak, G.L. and Hastay, J.H. (1974) *Biochim. Biophys. Acta* 348, 45—54
- 39 Yeagle, P.L., Hutton, W.C., Martin, R.B., Sears, B. and Huang, C. (1976) *J. Biol. Chem.* 251, 2110—2112
- 40 Lieber, M., Smith, B.T., Szakal, A., Nelson-Rees, W. and Todaro, G. (1976) *Int. J. Cancer* 17, 62—70
- 41 Zeitler, E. and Bahr, G.F. (1965) in *Quantitative Electron Microscopy* (Bahr, G.F. and Zeitler, E., eds.), p. 208, Williams and Wilkins, Baltimore
- 42 Zeitler, E. (1965) in *Quantitative Electron Microscopy* (Bahr, G.F. and Zeitler, E., eds.), p. 36, Williams and Wilkins, Baltimore
- 43 Marshall, A.T. (1975) in *Principles and Techniques of Scanning Electron Microscopy* (Hayat, M.A., ed.), Vol. 4, pp. 128—130

- 44 Marshall, A.T. (1975) in *Principles and Techniques of Scanning Electron Microscopy* (Hayat, M.A., ed.), Vol. 4, pp. 152—154
- 45 Marshall, A.T. (1975) in *Principles and Techniques of Scanning Electron Microscopy* (Hayat, M.A., ed.), Vol. 4, p. 140
- 46 Marshall, A.T. (1975) in *Principles and Techniques of Scanning Electron Microscopy* (Hayat, M.A., ed.), Vol. 4, p. 159
- 47 Coleman, J.R., Nilsson, J.R., Warner, R.R. and Batt, P. (1973) *Exp. Cell Res.* 76, 31—40
- 48 Somlyo, A.P., Somlyo, A.V., Devine, C.E., Peters, P.D. and Hall, T.A. (1974) *J. Cell Biol.* 61, 723—742
- 49 Wood, J.G. (1974) *J. Histochem. Cytochem.* 22, 1060—1063
- 50 Padawer, J. (1974) *J. Cell Biol.* 61, 641—648
- 51 Popescu, L.M. and Diculescu, I. (1975) *J. Cell Biol.* 67, 911—918
- 52 Isaacson, M.S. and Crewe, A.V. (1975) *Ann. Rev. Biophys. Bioeng.* 4, 137—184
- 53 Wall, J., Langmore, J., Isaacson, M. and Crewe, A.V. (1974) *Proc. Natl. Acad. Sci. U.S.* 71, 1—5
- 54 Verkleij, A.J., Zwaal, R.F.A., Roelofsen, B., Comfurius, P., Kastelijn, B. and van Deenen, L.L.M. (1973) *Biochim. Biophys. Acta* 323, 178—193
- 55 Finean, J.B. (1973) in *Form and Function of Phospholipids* (Ansell, D.B., Hawthorne, J.N. and Dawson, R.M.C., eds.), 2nd edn., pp. 188—190, Elsevier, Amsterdam
- 56 Grant, C.W.M., Wu, S.H.-W. and McConnell, H.M. (1973) *Biochim. Biophys. Acta* 363, 151—158